Neutron Generation from 10MeV Electron Beam to Produce Mo[99]

Borhani Zarandi, Mahmood[1*]; Tabbakh, Farshid[2]; Amrollahi Bioki, Hojjat[1]

[1] Atomic and Molecular Group, Faculty of Physics, Yazd University, Yazd, Iran

[2] Institutes of Nuclear Science and Technology, Tehran, Iran

Corresponding Email: mborhani@yazd.ac.ir

*Abstract- **In this paper MCNP4C code has been used to simulate of the photonuclear interaction induced by 10MeV electron beam is an approach for generating the high intensity neutrons. Since the results are depended on the target material, the calculations are performed for the targets made of high-z elements of Pb, Ta and W in a simple geometry**.*
Keywords: **Photonuclear Interaction, Rhodotron, Electron Beam, Photo-neutron**

I. Introduction

Except the nuclear reactors, the electron accelerators can be considered as the main source of neutron with some different specifications such as higher intensity, lower cost and much smaller size in compare with the nuclear reactors. On the other hand, isotope production method via (γ, n) reaction has more production yield [1] due to the wide range of neutrons energy beside the research reactors in which, the neutrons energy is in the thermal range. In this paper, we approach the both safety consideration and design related study for neutron generation using 10MeV electron beam.

Since most of the studies for producing the photo-neutrons are performed using electron with energy much more than 10MeV [2-8], the present work has concentrated on the results when the electrons with energy of 10MeV in a continuous beam impinge the target to generate the photo-neutron. The desired beam current is taken as 10mA obtained by an electron accelerator such as Rhodotron TT-200.

The MCNP4C [9] code is used to simulate the photonuclear interaction respecting the processed data provided by Los Alamos National Laboratory (LANL) and the Chinese Nuclear Data Center (CNDC) which are submitted to the IAEA Coordinated Research Project (CRP) on photonuclear data [10] in the ENDF-6 format and suitable for MCNP4C Monte Carlo codes. They are released as two libraries of "*lanl01u*" and "*cndc01u*" respectively. According to these processed data, the photonuclear cross sections for Tantalum and Lead are extracted from "*lanl01u*" library and for Tungsten from "*cndc01u*" library including the XSDIR file modification for corresponding elements. The photonuclear threshold energies and abundances of the related isotopes for these elements are presented in table1 [11] (Chadwick et al., 2000). As shown in this table, the elements of Lead, Tantalum and Tungsten have photo-neutron reaction threshold of around 8MeV, being suitable for generating neutrons with 10MeV e-beam. Beryllium, with resonances at 2MeV, can be alloyed with the target metal to convert the low energy photons to neutron.

In the following, we calculate the photo-neutron yield and flux corresponding to the targets materials and the geometry (target thickness) and then study the optimization of the target using the alloyed materials to obtain the maximum neutron yield and flux. The calculation consists of the energy distribution and the heat deposited in the targets too.

II. Material and Methodology

MCNP4C calculates the process of electron to photon conversion via Bremsstrahlung and photon to neutron as well. The geometry of the target is considered as simple as a cylinder with the radius of 5cm and the variable height (will be taken as the target thickness) along the z-axis that the beam impinge on one of its end.

The results are obtained under the variance reduction methods of *weight windows energy (wwe)*, *weight windows parameter (wwp)* and *cell-based weight windows bound (wwn1)* including tally type 5 with errors less than 5%. The energy depositions in the targets are calculated using tally type 6. The threshold energies presented in table1 are considered as the cutoff energy to decrease the computation time.

III. Results and Tables

The output files provide the statistical information by which, one can study many aspects such as, photon and neutron angular distribution and the reactions which cause to neutron, photon and electron creation and loss including their contributions. Also the output files illustrate that, almost 97% of the neutrons come from photonuclear reaction and the rests are belong to (n, xn) interaction.

In the following, we present more information for comparing our results to the experimental measurements or available standard data that can approve the reliability of the results. In a hight-z target, the ratio of electron energy lost via Bremsstrahlung to total energy lost (Bremsstrahlung + collisions) is given by the expression of $\left(\frac{(dE/\rho dx)_r}{(dE/\rho dx)_r+(dE/\rho dx)_c}\right)$, in where, $(dE/\rho dx)_r$ and $(dE/\rho dx)_c$ are mass radiative and mass collision stopping power respectively. According to the reference data [12] the corresponded values for 10MeV incident electrons for the mentioned elements are almost 0.5 and the MCNP4C outputs will lead us to the same value by dividing the Bremsstrahlung weight energy by summation of the both Bremsstrahlung and scattering weight energies.

Table 1 Photonuclear threshold energy and the isotopes abundances of Pb, Ta, W and Be [11]

Isotopes	(n, γ) Threshold Energy (MeV)	Abundance (%)
Pb-206	8.09	24.10
Pb-207	6.74	22.10
Pb-208	7.37	52.40
Ta-181	7.58	99.99
W-180	8.41	0.12
W-182	8.07	26.30
W-183	6.19	14.28
W-184	7.41	30.70
W-186	7.19	28.60
Be-9	1.67	100

In addition, the average energy of generated neutrons can be calculated by dividing the weight energy created by total weight produced for photo-neutrons in the targets [7]. Therefore, the neutrons average energies are 0.9MeV, 0.4MeV and 0.9MeV for Pb, Ta and W respectively.

Fig.1 shows the neutron yield per one incident electron in terms of Pb, Ta and W target thicknesses (with no Beryllium alloy) represented by the solid, dashed and dotted curves respectively. Increasing the target thickness will cause to increase the photo-neutrons yield. As one can see, at the optimal thicknesses of 8cm, 4cm and 2cm the corresponding curves find ignorable gradient. In other word, we can conclude the increasing the thickness more than optimal thickness will not affect the neutron yields. As illustrated in this figure, the neutron yield of 10^{12}neutron/s will be achieved for the beam current of 10mA.

Fig.2 shows the logarithmic scale of variation of the neutron flux along the beam direction, in terms of target thickness that represented by solid, dashed and dotted lines for Pb, Ta and W respectively (with no Beryllium alloy). For the current of 10mA, the maximum fluxes are in the order of 10^{12}n/cm^2/s and the thickness up to 8cm will cause to drop the flux to less than 10^{10} n/cm^2/s. As mentioned before, the more deviation from the center of the target will cause the less flux as well.
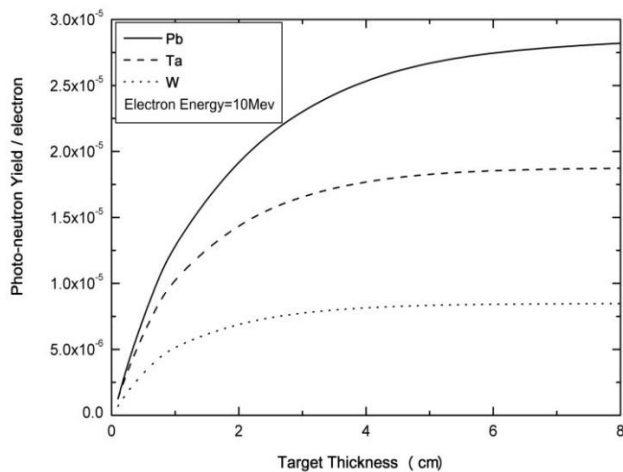

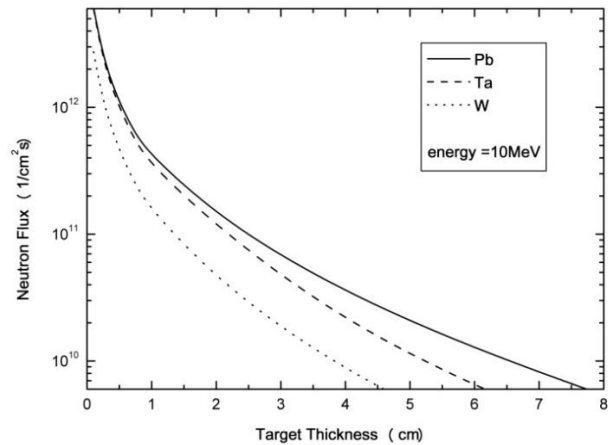Fig.1 The neutron yield in terms of target thickness for Pb, Ta and W.

Fig.2 The neutron flux in terms of thickness for Pb, Ta and W.

Fig.3 presents the neutron yield in terms of weight fraction of metal on Beryllium. As shown in this figure, for the value less than 50% (1 in horizontal axis), the neutron yield increases very sharp by increasing the metal weight fraction and for larger than 50% the decreasing is very smooth which indicates the sensitivity of neutron yield to the metal fraction. The targets with equal weight fractions (50% Be and 50% metal) will give the largest neutron yield. The maximum yields of 1.5×10^{13}n/s, 1.48×10^{13}n/s and 1.3×10^{13}n/s are obtained for W, Ta and Pb respectively. Therefore, the following calculations are performed based on 50% Beryllium and 50% metal as the optimum combination.
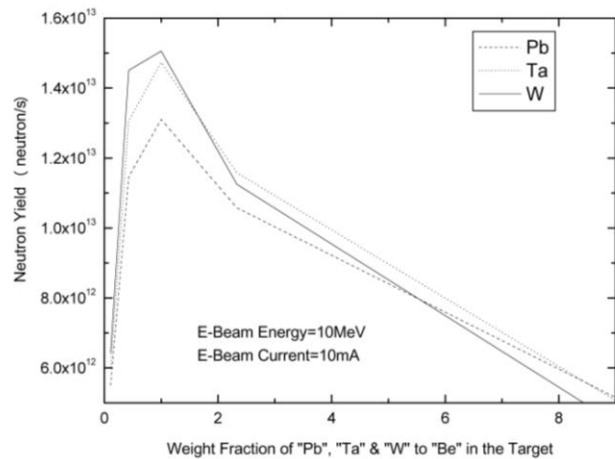

Fig.3 Neutron Yield in terms of weight fraction of "Ta", "W" and "Pb" in "Metal-Be" compound (E=10MeV and i=10mA).

Neutron flux as a function of target thickness is shown in Fig.4. Though, the neutron yield will increase when the target thickness increases, but, the flux will decrease as an order of magnitude. It can be seen that, at the point near the beginning of the target the flux will reach up to 2×10^{13}n/s/cm^2 as the maximum value of flux.
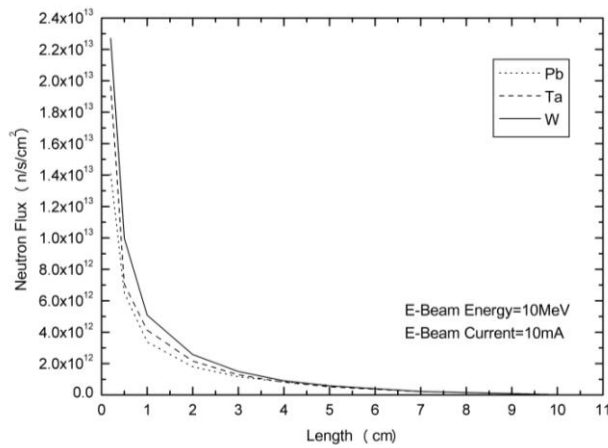
Fig.4 Neutron flux in the target along the beam direction
(E=10MeV and i=10mA).

Fig.5 shows the energy distribution of photo-neutrons in the target with the maximum distribution at energy of 1MeV. The related fluxes at this energy are 7×10^{12}n/s/cm^2, 1.05×10^{13}n/s/cm^2 and 1.2×10^{13}n/s/cm^2 for Pb, Ta and W respectively. As shown in the figure, the neutron energy extends to about 8MeV, it is because of the low Beryllium threshold of 1.67MeV. If the targets were Beryllium free referring to the table 1, the maximum energy of the neutrons could not exceed 3-4MeV regarding to the metals higher threshold energy for such interaction. The neutrons average energy also is about 0.8MeV as mentioned before.
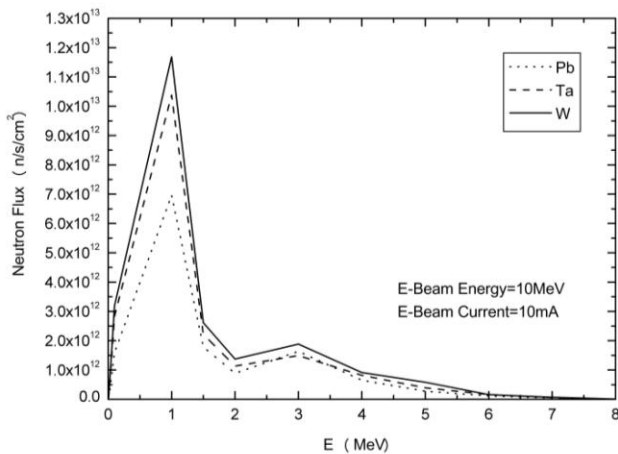

Fig.5 Energy distribution of the Photo-Neutrons and the related fluxes (E=10MeV and i=10mA).

Fig.6 shows the power deposited in unit of volume for different target volumes. The upper axis in this figure also represents the target thickness. As mentioned before the maximum distribution of the neutrons is along the beam axis therefore the power deposition calculation should be performed as a function of target thickness. The MCNP4C outputs show, the most contributions are belong to electrons and then to photons. Therefore, the curves in this Figure show the electron and photon contributions only.
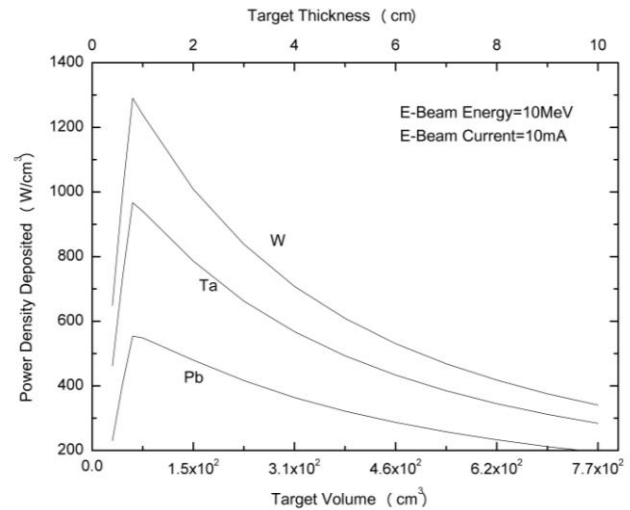

Fig.6 Power density deposited as a function of target volume (lower axis) and thickness (upper axis), when E=10MeV and i=10mA

As some applicable points of view, one can compare the activity value Mo-99 produced under electron beam to data obtained from reactors to evaluate the Rhodotron-TT200 as a neutron source and radioisotopes producer. To this purpose, DHRUVA-100MW reactor is considered[13] according to the following information: target: MoO_3 (90-120g per batch), neutron flux: 1.6×10^{14}n/s/cm^2, duration of irradiation: 1week and activity of Mo-99: 40Ci per batch.

Fig.7 shows the Rhodotron results when MoO_3 mass is 1.5g and 150g presented by black and red lines respectively. The cross section of (n, γ) reaction is $\sigma_{(n, \gamma)}$=0.13 ±0.005barn. As one can observe, after 1 week the Mo-99 activity will reach to the same activity as reactor data represented by dashed line. These data also are comparable to those obtained from TRR-5 research reactor [14].
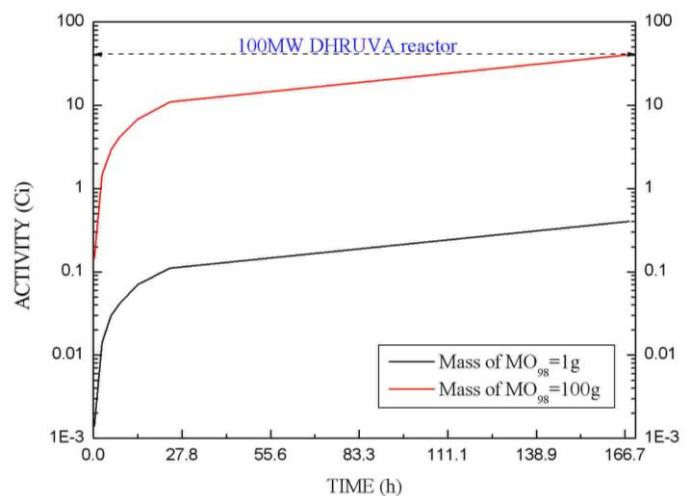

Fig.7 Mo-99 activity produced by Rhodotron-TT200 and 100MW DHRUVA reactor in terms of duration of irradiation

IV. Conclusion

In the previous section, the neutron generation via photonuclear and the related target specifications were studied for the electron beam with 10MeV energy. The

precision of the results obtained by calculation were evaluated by the both standard values and experimental measurements and it is found that, there are accommodation between these methods. Accordingly, the results corresponding to the photoneutron generation such as the yield, flux and heat deposition in targets have sufficient reliability to be applied the studies including safety related points of view of photon and neutron generation obtained under 10MeV electron beam and also the conceptual design of a neutron generator system using 10MeV electron accelerator that, the heat generated values present in this work will give some background for heat removal aspects.

References

i.   N.P. Dikiy, A.N. Dovbnya, V.L. Uvarov, Development of New Electron Irradiation Based Technology for Technetium-99m Production. Proceedings of Conference, Stockholm, Sweden, 1998, pp. 2389-2391.

ii.   G. N. Kim, H. S. Kang, J. Y. Choi, J. Accel. Plasma Res. 3 (1998) 9-17.

iii.   J. Chen, D. Beller, F. Harmon, and K. Sabourov, ISU Accelerator-Driven Sub-critical System Characterization, Transactions of American Nuclear Society, 93, Washington DC 2005, pp. 907-908.

iv.   V. C. Petwal, V. K. Senecha, K. V. Subbaiah. Pramana-journal of physics. 68 (2007) 235-241.

v.   R. Moreh, R.C. Block,Y. Danon. Nuclear Instrument and Methods in Physics Research A, 562 (2006) 401-406.

vi.   G. N. Kim, Y. S. Lee, D. Son, Photoneutron Spectrum at Pohang Neutron Facility Based on 100MeV Electron Linac. Proceeding of the particle accelerator conference, Chicago 2001, pp. 2542-2544.

vii.   M.C. White, a Brief Primer for Simulating Photonuclear Interactions with MCNP(X). X-5:MCW-00-89(U), Los Alamos National Laboratory, Los Alamos, NM (2000).

viii.   Y. Danon, R.C. Block, R. Testa, Medical Isotope Production Using a 60MeV Linear Electron Accelerator. ANS national meeting, Anaheim, CA, NS Transaction, 98 2008, pp. 894-895.

ix.   J. F. Briesmeister, Ed., MCNP - A General Monte Carlo N-Particle Transport Code, Version 4C, Los Alamos National Laboratory report, LA-13709-M (2000).

x.   M. B. Chadwick, A. I. Blokhin, T. Fukahori, IAEA-TECDOC-1178: Handbook of photonuclear data for applications. Cross section and spectra, IAEA Vienna, (2000).

xi.   R.K. Bull, International Journal of Radiation Applications and Instrumentation Part D, 11 (1986) 273.

xii.   IAEA-TECDOC-1340, Manual for reactor produced radioisotopes, IAEA, Vienna, 2003.